

See discussions, stats, and author profiles for this publication at: <https://www.researchgate.net/publication/21673622>

Blood viscosity in tube flow: Dependence on diameter and hematocrit

Article in American Journal of Physiology-Legacy Content · December 1992

DOI: 10.1152/ajpheart.1992.263.6.H1770 · Source: PubMed

CITATIONS

724

READS

3,689

3 authors, including:



Axel R Pries

Charité Universitätsmedizin Berlin

344 PUBLICATIONS 22,983 CITATIONS

[SEE PROFILE](#)



Peter A.L. Gaehtgens

Freie Universität Berlin

201 PUBLICATIONS 11,601 CITATIONS

[SEE PROFILE](#)

Blood viscosity in tube flow: dependence on diameter and hematocrit

A. R. PRIES, D. NEUHAUS, AND P. GAEHTGENS

Freie Universität Berlin, Department of Physiology, D-1000 Berlin 33, Federal Republic of Germany

Pries, A. R., D. Neuhaus, and P. Gaehtgens. Blood viscosity in tube flow: dependence on diameter and hematocrit. *Am. J. Physiol.* 263 (*Heart Circ. Physiol.* 32): H1770-H1778, 1992.—Since the original publications by Martini et al. (*Dtsch. Arch. Klin. Med.* 169: 212-222, 1930) and Fahraeus and Lindqvist (*Am. J. Physiol.* 96: 562-568, 1931), it has been known that the relative apparent viscosity of blood in tube flow depends on tube diameter. Quantitative descriptions of this effect and of the dependence of blood viscosity on hematocrit in the different diameter tubes are required for the development of hydrodynamic models of blood flow through the microcirculation. The present study provides a comprehensive data base for the description of relative apparent blood viscosity as a function of tube diameter and hematocrit. Data available from the literature are compiled, and new experimental data obtained in a capillary viscometer are presented. The combined data base comprises measurements at high shear rates ($\bar{u} \geq 50 \text{ s}^{-1}$) in tubes with diameters ranging from 3.3 to 1,978 μm at hematocrits of up to 0.9. If corrected for differences in suspending medium viscosity and temperature, the data show remarkable agreement. Empirical fitting equations predicting relative apparent blood viscosity from tube diameter and hematocrit are presented. A pronounced change in the hematocrit dependence of relative viscosity is observed in a range of tube diameters in which viscosity is minimal. While a linear hematocrit-viscosity relationship is found in tubes of $\leq 6 \mu\text{m}$, an overproportional increase of viscosity with hematocrit prevails in tubes of $\geq 9 \mu\text{m}$. This is interpreted to reflect the hematocrit-dependent transition from single- to multifile arrangement of cells in flow.

hemorheology; Fahraeus-Lindqvist effect; blood viscosity

IT HAS BEEN KNOWN for a long time that apparent blood viscosity depends not only on hematocrit, plasma protein concentration, and temperature but also on the shear forces applied and the geometry of the instrument in which it is measured. Martini et al. (33) as well as Fahraeus and Lindqvist (16) were the first to observe a significant decrease of apparent blood viscosity in tubes with diameters ranging between ~ 500 and $50 \mu\text{m}$. This reduction in apparent blood viscosity, which has been named Fahraeus-Lindqvist effect, is especially relevant if measurements of apparent viscosity are to be applied to blood flow through the vascular system. Blood vessels exhibit diameter variations over four orders of magnitude ranging from $\sim 3 \text{ cm}$ in the large systemic vessels down to $3 \mu\text{m}$ in skeletal muscle capillaries.

The Fahraeus-Lindqvist effect was confirmed in vitro by a large number of investigators (2, 4-8, 10, 19, 21-23, 25, 34, 41-43, 51, 54) who demonstrated that the decrease of apparent blood viscosity continues down to diameters of $\sim 10 \mu\text{m}$. For even smaller diameters approaching the minimum cylindrical diameter of normal human erythrocytes ($\sim 2.7 \mu\text{m}$), Gerbstadt et al. (21) and Gaehtgens (19) reported a steep increase of viscosity. Empirical descriptions of blood viscosity as a function of tube diameter were derived based on compilations of literature data (19, 30, 37, 40, 55). Such

compilations are a prerequisite for the development and use of hydrodynamic models of the cardiovascular system and especially of the terminal vascular bed, since the contribution of different size microvessels to total peripheral resistance is strongly affected by diameter-dependent variation of blood viscosity. Hydrodynamic models of vascular perfusion have proved to be important tools, allowing a correlation of data obtained from whole organ studies with those derived from single microvessels (17, 18, 26, 31, 36, 37, 40, 44, 48, 55).

However, earlier data compilations were derived from too limited data material and provide fitting algorithms that do not adequately represent all features of the experimental data. Furthermore, the analysis of the hematocrit dependence of apparent viscosity in different size tubes was hitherto limited by the paucity of available data for wide hematocrit ranges. In the present report, an attempt is therefore made to provide a comprehensive quantitative description of viscosity measurements available in the literature. In addition, new experimental data are presented to obtain a more complete data set relating apparent blood viscosity to vessel diameter in a wider range of hematocrits. In this context, only data obtained at high shear rates ($\bar{u} \geq 50 \text{ s}^{-1}$) are considered. This may be justified for a first approximation to blood flow in the microcirculation for at least two reasons. 1) The influence of shear rate on viscosity appears to be small in the shear rate range existing in the microcirculation under normal conditions. Pseudo-shear rates (\bar{u} , i.e., mean blood velocity divided by vessel diameter) generally range above 50 s^{-1} (32), whereas significant effects of shear rate on viscosity, at least in tube flow, are to be expected at substantially lower \bar{u} (43). 2) The shear rate dependence of blood is influenced by several additional factors, the importance of which for microcirculatory perfusion is not easily assessed. It has been shown that the increase of viscosity in low-shear-rate tube flow is strongly affected by cell sedimentation (9, 13, 42) and is further complicated by the effect of erythrocyte aggregation tendency. In addition, transit times of blood through the vessel segments of microcirculatory networks under normal flow conditions are probably shorter than required for the development of cell aggregation and sedimentation and thus of steady-state viscosity at low shear rates.

DATA BASE

Literature data. The data base used in this report comprises measurements of viscosity of blood or red cell suspensions from 15 studies in the literature. These measurements were carried out in a wide range of tube diameters (~ 3 - $2,000 \mu\text{m}$) and hematocrits up to 0.9 with different experimental methods (Tables 1 and 2). In addition, results of earlier viscosity measurements by two of the authors (Gaehtgens and Pries) and by Barbee and Cokelet (personal communication) that were not previously

Table 1. Methodological characteristics of viscosity measurements and relationship between apparent viscosity and hematocrit

Authors	Species	Sample (anticoagulant)	Temp., °C	Tube Diameter, μm	Tube Length, mm	Pseudo-Shear Rate, diam/s	Method of Flow Determination
<i>Viscosity measurements</i>							
Martini et al. (1930)	Human	Whole blood (Hirudin)	38	70300	24–194	1,900–800	Fluid-air meniscus in series-coupled pipette
Fahraeus & Lindqvist (1931)	Human	Whole blood (?)	38	40–505	13–127	>200	Fluid-air meniscus in series-coupled pipette
Bayliss (1952)	Dog	Defibrinated blood	Room (15–25)	14–139 (scaled)	~1.5–3	?	Fluid-air meniscus in series-coupled pipette
Haynes & Burton (1959)	Human	RBC (ACD)	25.5	114–944	>175·diam.	>200	Fluid-air meniscus in series-coupled pipette
Prothero & Burton (1962)	Human	Whole blood (ACD)	23.5	9.4	~1	>3,000	Size of droplet produced at capillary tip
Gerbärdt et al. (1966)	Human	Whole blood (heparin)	20	4.2–70	~2,500·diam	120–300	Fluid-fluid meniscus in series-coupled pipette
Braasch & Jenett (1968)	Pig	Defibrinated blood	Room (22)	5.6–47 (scaled)	~1–2	100–400	Pressure created by outflow in sealed chamber, oscillating flow
Halikas & Sheppard (1969)	Dog	Whole blood (mepesulfate, heparin)	38	107–550 (scaled)	34–205	250–900	Fluid-air meniscus in series-coupled pipette
Azelvandre & Oiknine (1976)	Human	RBC in saline	20	58–1978	~30	>250	Fluid-air meniscus in series-coupled pipette
Gupta & Seshadri (1977)	Human	RBC in saline	31	86–444	75–82	>50	Fluid-air meniscus in series-coupled pipette
Voss (1983)	Human	RBC in saline	37	34–95	~1,000·diam	180–140	Pressure created by outflow in sealed chamber
Reinke et al. (1986)	Human	Whole blood (EDTA)	Room (26)	31–94	35–65	~50	Fluid-fluid meniscus in series-coupled pipette
Reinke et al. (1987)	Human	Whole blood (EDTA)	Room (26)	31–132	38–73	100	Fluid-fluid meniscus in series-coupled pipette
McKay & Meiselman (1988)	Human	RBC in saline	21	33–146	~65	630–420	Flow imposed by syringe, pressure difference measured
Stadler et al. (1990)	Human	RBC in plasma (EDTA)	37	50–500	10–100	>100	Fluid-air meniscus in series-coupled pipette
Barbee & Cokelet, personal commun	Human	Whole blood (ACD)	23	29–99	200–380	~90	Flow imposed by syringe, pressure difference measured (Barbee and Cokelet, 1971)
Gaehgens & Pries, personal commun	Human	RBC in saline	Room (24)	3.3–6	~4	>50	Optical measurement of RBC and plasma velocity (Albrecht et al., 1979)
Present data	Human	RBC in plasma (EDTA)	Room (20–23)	9–40	6–11	>200	Fluid-air meniscus in series-coupled tube
<i>Apparent viscosity and hematocrit</i>							
Whittaker & Winton (1933)	Dog	Whole blood defibrinated	37	930	303	~150	Sampling of tube outflow
Barbee (1973)	Human	Whole blood (ACD)	23, 37	811	280	100	Flow imposed by syringe, pressure difference measured
Brooks et al. (1970)	Human	RBC in saline	25			(170.8 s ⁻¹)	Rotational viscometer, Coaxial cylinder type
Chien et al. (1971)	Human	RBC in saline	37			(52 s ⁻¹)	Rotational viscometer, coaxial cylinder type

RBC, erythrocytes; ACD, acid-citrate-dextrose.

published in the present form are included.

The viscosity of blood during tube flow is strongly correlated with the volume concentration of erythrocytes within the tube, the tube hematocrit (Hct_T). However, in most studies Hct_T was not measured, the known parameter being the feed hematocrit (Hct_F). For the typical experimental setups used, it can be assumed that the volume concentration of the blood entering or leaving the capillary tube (discharge hematocrit, Hct_D) equals Hct_F , because phase-separation effects excluding erythrocytes from the capillary are absent. This holds for experimental conditions in which the flow across the entrance of the capillary tube that results from stirring the feed reservoir is slow compared with that in the capillary (39). In some studies (e.g., Ref. 51) the equality of Hct_D and Hct_F was actually demonstrated by sampling the outflow of the capillary tube.

It is known that Hct_T is reduced compared with Hct_D (15). This hematocrit reduction (Fahraeus effect) depends mainly on tube diameter and hematocrit. In the following, all viscosity measurements are related to Hct_D , which is taken to be identical

to Hct_F in those data sets in which discharge hematocrit was not explicitly stated.

Three of the literature studies analyzed have been performed with blood from species (pig, dog) other than humans. Because the mean red cell volume (MCV) of these species differs from that found in humans, the tube diameters given in these reports were scaled using the cube root of the ratio of the respective MCVs. This recognizes the fact that apparent blood viscosity is closely related to the cell-to-tube diameter ratio (λ).

Some references that have been included in previous compilations (19, 30) are not included in the present data base. Jay et al. (28) used a conical measuring capillary, which may have caused uneven hematocrit distribution along the tube. In the studies of Barras (5–7), the viscosity reported from measurements in tubes with diameters of 1 mm is significantly lower than that measured in rotational viscometers, whereas in tubes of ~5-mm diameter the viscosity is much higher. Although specific reasons for these discrepancies are not clear, these data have not been included.

Table 2. Statistical results for dependence of apparent blood viscosity on hematocrit

Authors	<i>D</i> , μm	<i>n</i>	Hct_D		<i>B</i>	<i>C</i>	<i>r</i> ²	<i>r</i> ² (linear)
			min	max				
Gaehtgens & Pries	3.3	72	0	0.33	12.29	-0.431	0.852	0.844
Gaehtgens & Pries	4.4	96	0	0.65	-0.80	1.539	0.776	0.769
Gaehtgens & Pries	5.6	44	0	0.36	-0.42	3.850	0.773	0.737
Gaehtgens & Pries	6	170	0	0.63	-0.49	2.66	0.533	0.505
Present data	9	45	0	0.87	0.62	-0.879	0.937	0.589
Present data	12	54	0.03	0.89	0.36	-1.299	0.948	0.512
Present data (medium viscosity 1.85 cP)	20	59	0.05	0.8	0.86	-0.908	0.935	0.731
Present data (medium viscosity 5.5 cP)	20	67	0.03	0.84	0.91	-0.814	0.968	0.723
Present data (medium viscosity 9 cP)	20	37	0.05	0.8	1.41	-0.599	0.926	0.788
Bayliss (1952)	26	10	0.05	0.9	1.15	-0.988	1.000	0.570
Reinke et al. (1986)	31	8	0.12	0.64	1.07	-0.907	0.986	0.799
Present data	40	64	0.03	0.8	1.16	-0.930	0.975	0.726
Reinke et al. (1986)	41	13	0.15	0.65	1.31	-0.930	0.962	0.679
Bayliss (1952)	55	10	0.05	0.9	3.54	-0.743	1.000	0.645
Barbee & Cokelet	75	7	0.18	0.59	2.10	-0.801	0.999	0.864
Reinke et al. 1986	94	5	0.2	0.59	2.53	-0.749	0.975	0.850
Barbee & Cokelet	99	7	0.15	0.55	2.15	-0.875	0.997	0.894
Barbee & Cokelet	128	5	0.23	0.545	2.04	-0.851	0.996	0.870
Barbee & Cokelet	153.5	7	0.2	0.54	2.86	-0.769	0.998	0.892
Barbee & Cokelet	221	4	0.2	0.65	3.18	-0.721	0.995	0.843
Barbee & Cokelet	811	9	0.12	0.59	2.92	-0.808	0.997	0.876
Barbee (1973)	811	15	0.12	0.59	2.83	-0.813	0.996	0.886
Whittaker & Winton (1933)	930	Not given	0.05	0.8	1.49	-0.835	0.996	0.881
Whittaker & Winton (1933)	930		0	0.84	3.46	-0.778	0.996	0.767
Brooks et al. (1970)	Rotational viscometer	11	0.08	0.70	4.15	-0.900	0.991	0.826
Chien et al. (1971)	Rotational viscometer	6	0.25	0.93	9.12	-0.733	0.975	0.488

D, tube diameter; Hct_D , discharge hematocrit; *B*, steepness; *C*, curvature; r^2 , correlation coefficient.

The absolute apparent viscosities given in the literature reports show a high degree of variability even at a given tube diameter and hematocrit. This can in part be attributed to the variation of suspending medium viscosity used, which covers a 2.5-fold range between different studies. Therefore data were corrected for medium viscosity by calculating a relative apparent blood viscosity (η_{rel}). If medium viscosity was not given in a study, the respective value was deduced from the type of medium used (e.g., saline) and the temperature. Corrections for temperature were not made, since η_{rel} is supposed to be independent of temperature (3).

Experimental data. The present study also includes new experimental data obtained by tube flow viscometry in glass capillaries with diameters between 9 and 40 μm at hematocrits between 0.05 and 0.89. The capillary viscometer was described in detail elsewhere (35). In brief, the viscometer (Fig. 1) consisted of a small (2 ml) reservoir connected to the vertical glass capillary (length between 6 and 11 mm). The exit orifice of the capillary was connected to one end of a horizontal measuring tube with an inner diameter 10–20 times larger than that of the capillary. The other end of the measuring tube was connected to negative-pressure source and a mercury manometer. The system was initially filled with isotonic degassed saline, which was then replaced in the reservoir by the sample to be analyzed.

For measurement of viscosity, a negative pressure (between -100 and -300 mmHg) was applied and the advancement of the saline-air meniscus in the measuring tube per time recorded with a stereomicroscope. With each sample, at least six determinations of meniscus velocity were made at each driving pressure, and at least three different driving pressures were employed. Results were averaged for calculation of viscosity. Plasma perfusion always preceded a perfusion with a red cell suspension.

Human venous blood was obtained by venipuncture from healthy donors and anticoagulated with EDTA (2.5 mg/ml).

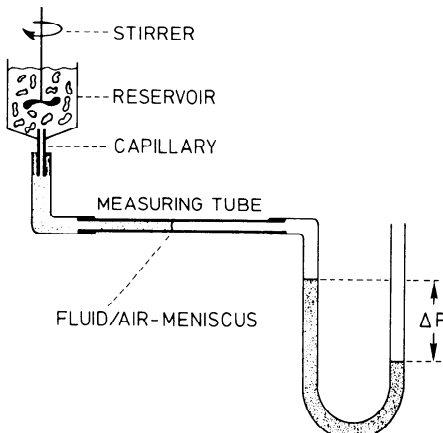


Fig. 1. Capillary viscometer setup. Vertical capillary is perfused from a feeding reservoir by applying a negative pressure to downstream end of horizontal measuring tube. Advancement of fluid-air meniscus in measuring tube is recorded per unit time. Comparison of meniscus velocity measured at identical driving pressures for plasma, and red cell suspension to be tested yields values of relative apparent viscosity.

Erythrocytes were washed with buffered saline and resuspended in autologous plasma at hematocrits up to 0.89. From each blood sample, at least six suspensions with different hematocrits were prepared. Additional cell suspensions were prepared in which the suspending medium viscosity was elevated from 1.85 cP to 5.5 and 9.0 cP (values measured at room temperature), respectively, by addition of dextran (40,000 mol wt) to the plasma. The red cell suspension in the reservoir was gently stirred to prevent erythrocyte sedimentation. The relative apparent viscosity of the red cell suspensions was obtained by dividing the meniscus velocity obtained with plasma by that determined with the red cell suspension at the same pressure head.

The perfusion pressures chosen provided shear rates exceeding 200 s^{-1} even for the high hematocrit samples. Systematic variations of relative viscosity with $\dot{\gamma}$ were not observed. All measurements were carried out at room temperature ($20\text{--}23^\circ\text{C}$).

DATA PRESENTATION AND ANALYSIS

Diameter dependence. A total of 163 original values of relative apparent viscosity of red cell suspensions obtained from the 18 studies (Table 1) are shown in Fig. 2. These measurements were made at Hct_F between 0.4 and 0.45. If Hct_F was <0.45 , the viscosity was extrapolated to a hematocrit of 0.45.

$$\eta_{\text{rel}\,0.45} = 1 + (\eta_{\text{rel}} - 1) \cdot (0.45/\text{Hct}_F) \quad (1)$$

The data demonstrate a consistent trend according to the Fahraeus-Lindqvist effect. $\eta_{\text{rel}\,0.45}$ reaches a value of ~ 3.2 at tube diameters of $>1,000 \mu\text{m}$, which is in agreement with the values obtained in rotational viscometers (11, 12). In tubes with diameters of $<1,000 \mu\text{m}$, $\eta_{\text{rel}\,0.45}$ decreases with decreasing diameter. The lowest values of $\eta_{\text{rel}\,0.45}$ (~ 1.25) are found at tube diameters of $\sim 7 \mu\text{m}$. This statement is, however, based on the results of only four studies, and only one of these (21) allows a direct

determination of the viscosity minimum because of the diameter range covered. The paucity of data in this range reflects the experimental difficulties encountered in perfusion studies with tube diameters of capillary dimensions.

A number of analytical approaches have been developed to describe the variation of η_{rel} with tube diameter. In some of these approaches blood flow is modeled by assuming a cell-rich core surrounded by a marginal cell-poor layer (14, 24, 45, 53, 56), whereas others assume a number of concentric, unsheared laminae of finite size (24, 29). Secomb and co-workers (46, 47, 49) used the lubrication theory to model apparent blood viscosity under single-file conditions, whereas Barbee and Cokelet (4) deduced the changes in apparent viscosity from changes in Hct_T relative to the hematocrit in the feed reservoir. Each of these models provides predictions for a limited diameter range only (30), and a comprehensive theory for a larger diameter and hematocrit range still seems to be lacking.

Therefore a purely empirical fit appears to represent the best way to describe the experimental data and to allow application of the results to model simulations of

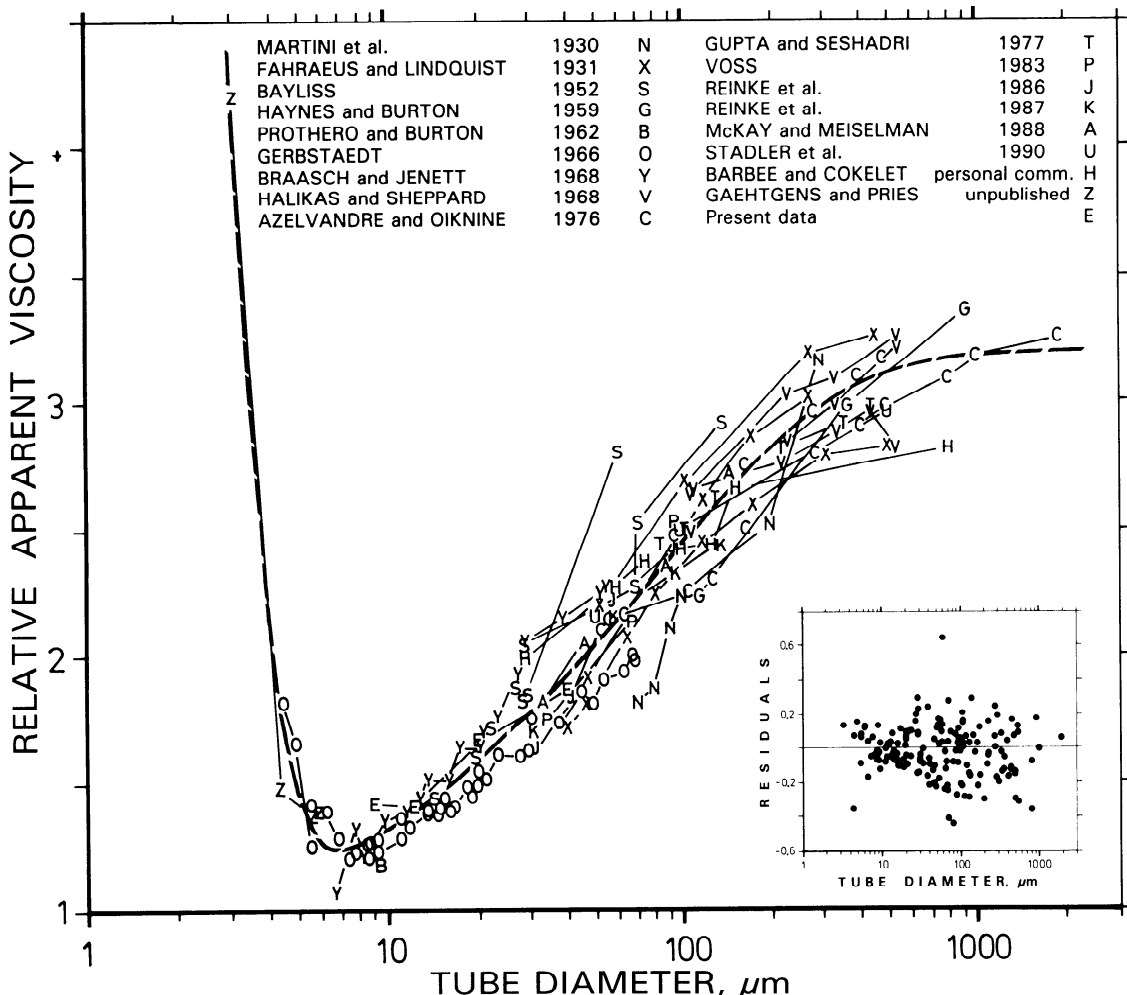


Fig. 2. Relative apparent viscosity (η_{rel}) of red cell suspensions with a hematocrit of 0.45 perfused through glass tubes with inner diameters between 3.3 and $1,978 \mu\text{m}$. Experimental conditions of studies cited are given in Table 1. In addition to original data, a fitting line according to Eq. 2 is given. Residuals of experimental data to values predicted are shown in inset.

blood flow through vascular beds. In such a fit, the residual variance of experimental data from an arbitrary function is minimized and the parameters of the function generally have no specific physical meaning. In the present study, a combination of two exponential equations was used, in which the first term dominates the increase of viscosity with decreasing tube diameter ($D, \mu\text{m}$) in the range below $\sim 7 \mu\text{m}$, and the following two terms govern the fit to the viscosity data at higher tube diameters

$$\eta_{\text{rel} 0.45} = 220 \cdot e^{-1.3D} + 3.2 - 2.44 \cdot e^{-0.06D^{0.645}} \quad (2)$$

This equation was designed to asymptotically approach, with increasing diameter, a preset viscosity value at infinite tube diameter, to show a minimum in an intermediate diameter range and a steep increase in the smallest tubes. An asymptotic increase of viscosity to infinity for vessel diameters approaching the theoretical minimum cylindrical cell diameter ($2.7 \mu\text{m}$) was not attempted, since such a behavior of the equation did not allow an optimal fit of the available data at the low end of the diameter scale. This might be due to the fact that a fixed-diameter threshold estimated from averaged quantities of red cell volume and surface area underestimates the influence of the large variability of these parameters within the cell population of a given blood sample. Even a small fraction of large erythrocytes might lead to a substantial increase of viscosity in tubes that are much larger than the idealized theoretical minimum cylindrical cell diameter.

The numerical parameters of the final fit were adjusted interactively on the basis of the correlation coefficient of the fit and its residuals (Fig. 2). An automatic nonlinear regression procedure was not used, since the number of available data points is not uniformly distributed in the diameter range. In addition, in the low tube diameter range the number of data points given in the individual studies differs strongly. The r^2 value reached for the final fit of the data was 0.919 ($n = 163$).

Hematocrit dependence. In rotational viscometers, apparent blood viscosity increases in an nonlinear fashion with hematocrit (11, 12). A qualitatively similar behavior is found in glass tubes down to a diameter of $\sim 9 \mu\text{m}$ (Fig. 3). In even smaller tubes, however, the relationship between viscosity and hematocrit seems to be linear, at least in the experimentally investigated range. To account for these differences in a parametric mathematical description, it is necessary to include a term reflecting the shape of the viscosity dependence on hematocrit and its variation with vessel diameter. However, the data base describing the hematocrit dependence of apparent viscosity is much smaller than that used to estimate the parameters of the diameter dependence. Although a number of authors provide viscosity values for more than one hematocrit, the range of hematocrits covered and/or the number of samples with different hematocrits is too low in many cases. Results of some studies were not utilized in the present analysis, since the cell suspensions were obtained from patients exhibiting largely differing systemic hematocrits (e.g., Ref. 38). In addition, data obtained in Ostwald viscometers (e.g., Ref. 52) were not

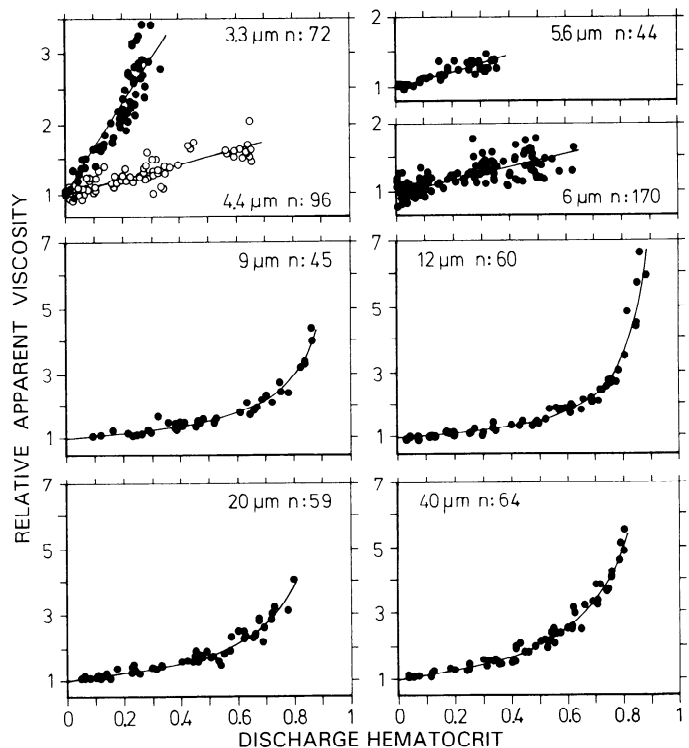


Fig. 3. η_{rel} as a function of hematocrit of red cell suspensions perfused through glass tubes of different diameters. Experimental data shown for tubes with diameters of $>6 \mu\text{m}$ have been obtained in present study; data for smaller tubes represent earlier measurements by Gaehtgens and Pries. Continuous lines represent fits to data using Eq. 3 together with B and C values from Table 2.

included, since the shear rates in this instrument are rather low and in turn depend on viscosity, which could have resulted in an overestimation of the viscosity increase with increasing hematocrit.

Using the present experimental results as well as those available in the literature (Table 1), we found that a consistently satisfying description of the hematocrit-viscosity relationship was obtained with the following equation

$$\eta_{\text{rel}} = 1 + B \cdot [(1 - \text{Hct}_D)^C - 1] \quad (3)$$

In this equation, the parameter C describes the curvature of the relationship between relative apparent blood viscosity and hematocrit. A value of 1 corresponds to a linear dependence, whereas values of <1 indicate a convex shape of the relationship toward the abscissa, as generally described for larger tubes or rotational viscometers. By use of an iterative procedure maximizing the correlation coefficient (r^2) between measured and predicted values, C was optimized for each data set analyzed (Table 2). For tube diameters between 3.3 and $6 \mu\text{m}$, the values of r^2 obtained upon optimization of C showed no statistically significant difference from those for a linear relationship (r^2 linear). Therefore capillaries in that diameter range were assigned a C value of 1. The resulting values of C are plotted as a function of tube diameter in Fig. 4 along with values calculated for data obtained in rotational viscometers.

The data shown in Fig. 4 indicate a rapid transition from a linear ($C \sim 1$) to a convex shape of the viscosity-hematocrit relationship in the diameter range between

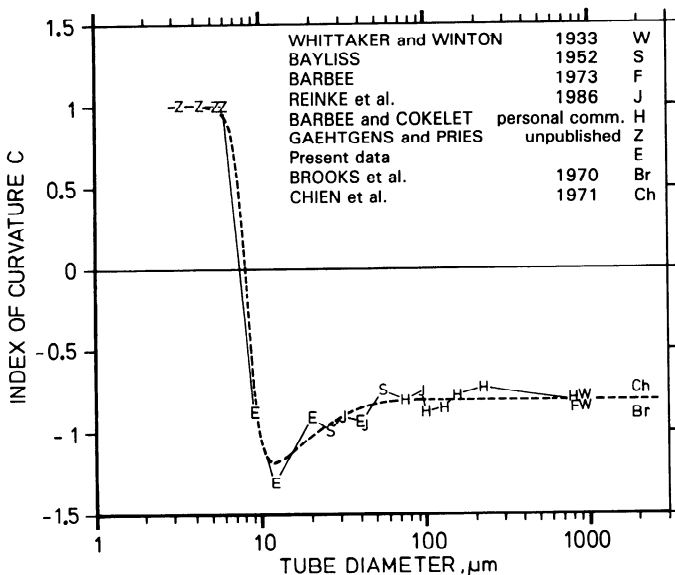


Fig. 4. Variation of parameter C , which describes curvature of relationship between η_{rel} and hematocrit with tube diameter. Predictions of an empirical fit according to Eq. 4 are shown along with values determined for present experimental data and those from literature.

6 and 9 μm . For tube diameters in the range of 10–30 μm there seems to be an especially strong increase of viscosity with hematocrit, whereas for even larger diameters the C values approach those found in rotational viscometers under comparable conditions.

To allow an implementation of these findings into a description of apparent blood viscosity as a function of vessel diameter and hematocrit, the relation between

C and diameter D (in μm) was fitted by an empirical equation

$$C = (0.8 + e^{-0.075D}) \cdot \left(-1 + \frac{1}{1 + 10^{-11} \cdot D^{12}} \right) \quad (4)$$

$$+ \frac{1}{1 + 10^{-11} \cdot D^{12}}$$

Combined dependence of viscosity on diameter and hematocrit. To allow a combined description of apparent blood viscosity as a function of both vessel diameter and hematocrit, Eq. 2 was used to derive diameter-dependent values for the parameter B of Eq. 3. According to Eq. 3, the relative viscosity for a hematocrit of 0.45 ($\eta_{\text{rel} 0.45}$) is given as

$$\eta_{\text{rel} 0.45} = 1 + B \cdot [(1 - 0.45)^C - 1] \quad (5)$$

This equation can be solved for B to give

$$B = \frac{\eta_{\text{rel} 0.45} - 1}{(1 - 0.45)^C - 1} \quad (6)$$

Substitution of Eq. 6 into Eq. 3 results in

$$\eta_{\text{rel}} = 1 + (\eta_{\text{rel} 0.45} - 1) \cdot \frac{(1 - \text{Hct}_D)^C - 1}{(1 - 0.45)^C - 1} \quad (7)$$

Numerical values for $\eta_{\text{rel} 0.45}$ and C for a given diameter may be obtained from Eqs. 2 and 4, respectively. Predictions of relative apparent blood viscosity based on this procedure are compared in Fig. 5 with experimental values for the Hct_D levels of 0.2, 0.45, and 0.60.

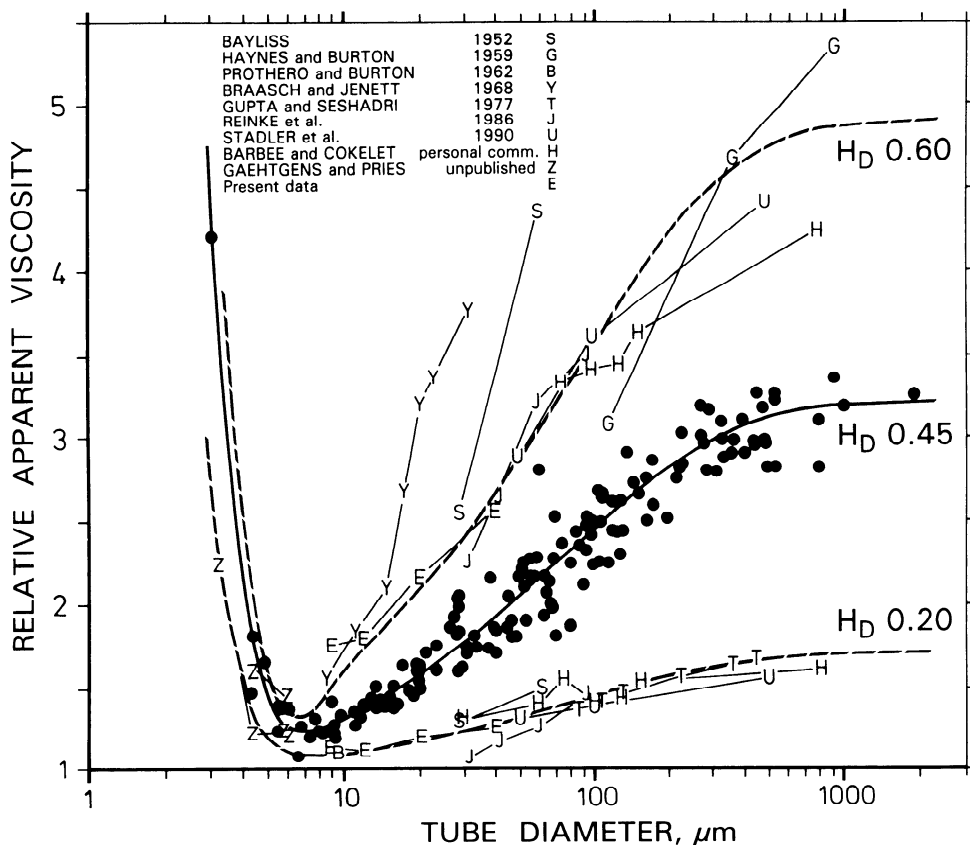


Fig. 5. η_{rel} of red cell suspensions perfused through tubes of different diameters. ● and fitting line for a hematocrit of 0.45 correspond to data given in Fig. 1. Experimental data reported for hematocrits of 0.2 and 0.6 are shown along with predictions (broken lines) from Eq. 7.

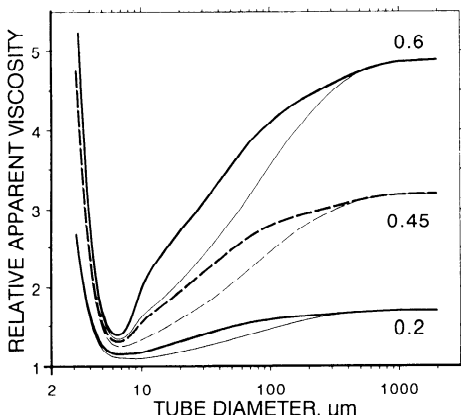


Fig. 6. η_{rel} as a function of tube diameter. Data for fixed tube hematocrits (heavy lines) are compared with values for fixed discharge hematocrits (thin lines) to illustrate impact of Fahraeus effect on η_{rel} .

If the fitting equations presented here are to be used in applications in which Hct_T , but not Hct_D , is known, empirical information on the Fahraeus effect and its dependence on tube diameter and hematocrit must be used. In the present context, a previously compiled (40) parametric description of the Fahraeus effect is used

$$\frac{\text{Hct}_T}{\text{Hct}_D} = \text{Hct}_D + (1 - \text{Hct}_D) \cdot (1 + 1.7 \cdot e^{-0.35D} - 0.6 \cdot e^{-0.01D}) \quad (8)$$

In the following, the numeric term will be replaced by

$$X = 1 + 1.7 \cdot e^{-0.35D} - 0.6 \cdot e^{-0.01D} \quad (9)$$

for reasons of simplicity. Equation 8 can be solved for Hct_D using standard procedures

$$\text{Hct}_D = -\frac{X}{2 - 2X} + \left[\left(\frac{X}{2 - 2X} \right)^2 + \frac{\text{Hct}_T}{1 - X} \right]^{0.5} \quad (10)$$

to allow the calculation of apparent relative viscosity using the fitting algorithms presented here. The results of such calculations are shown in Fig. 6 in which the dependence of viscosity on diameter is compared for three fixed Hct_T levels with that given in Fig. 5 for Hct_D .

DISCUSSION

The experimental data of apparent blood viscosity derived from the literature for a hematocrit of 0.45 show remarkable agreement despite the large variability of suspension media and experimental conditions of measurement (Table 1). The composition of suspensions in the data sets presented here ranges from anticoagulated whole blood to washed erythrocytes in saline, the temperatures between 15 and 30°C, and the viscosity of the suspending medium from 0.69 to 1.93 cP. As obvious from Fig. 2, these differences seem to exert no major effect on relative viscosity for a hematocrit of 0.45. The effects of temperature and medium viscosity were quantified by analyzing the deviation of the individual data points from the fitting line according to Eq. 2 (Fig. 2). The regression of these residuals against temperature and medium viscosity yielded extremely weak correlations, with slopes of -0.005 for the dependence on temperature (in °C)

and 0.069 for the dependence of η_{rel} on medium viscosity (in cP). The corresponding correlation coefficients ($r^2 = 0.052$ and 0.036, respectively) indicate that only ~5% of the residual variance of viscosity can be explained by these factors. It therefore appears to be justified for a large range of experimental conditions (temperature, blood composition) to calculate apparent blood viscosity from the relative viscosity as given here and the viscosity of the suspending medium used.

A minor but systematic effect of medium viscosity was, however, found in the shape of the relation between η_{rel} and Hct_D in the experiments in which the viscosity of the suspending medium was deliberately elevated from 1.85 cP to 5.5 and 9 cP, respectively (Table 2). Although η_{rel} at a hematocrit of 0.45 showed no systematic changes under these conditions, the C value increased from -0.901 to -0.814 and -0.599, respectively, with increasing suspending medium viscosity indicating more linear relations between viscosity and hematocrit at high medium viscosities.

The diameter dependence of blood viscosity is indirectly related to the λ (the cell-to-tube diameter ratio). This is true for both the steepness (B in Eq. 3) and the curvature (C in Eq. 3) of the relation between η_{rel} and hematocrit. The relative amount of energy dissipation due to cell-cell interactions in the central flow regions decreases with increasing λ , whereas the impact of the marginal cell poor flow regions on apparent viscosity increases. This leads to a continuous decline of $\eta_{\text{rel},0.45}$ with decreasing tube diameter starting at diameters of ~1,000 μm down to a diameter range in which the deformation of erythrocytes is limited because of their surface area and volume ratio. At even smaller tube diameters, the thickness of the lubricating plasma layer around the erythrocyte core decreases and the apparent blood viscosity starts to increase (48).

The changes of the curvature index C with decreasing tube diameter probably reflect the transition from multi-file flow conditions found in larger tubes to the single-file conditions in small capillaries. Under multi-file flow conditions, addition of erythrocytes to the flowing blood leads to an overproportional increase of the energy dissipation due to augmented cell-cell interactions. This leads to a strong curvature of the relation between η_{rel} and Hct_D and a low value of C . In single file flow, which occurs in small tubes with high values of λ , however, interactions between individual erythrocytes are minimal at low hematocrits and each additional erythrocyte leads to a finite increase of total pressure drop along the vessel. Therefore the relation between hematocrit and blood viscosity is linear (50). At higher hematocrits, the stacked-coin model (50) predicts a less than proportional increase of η_{rel} due to plasma trapping between erythrocytes. The overall shape of the viscosity-hematocrit relationship should therefore be bent away from the abscissa, yielding curvature indexes of >1. Such a tendency was in fact found in capillaries with diameters between 6 and 4.4 μm (Table 2). However, the limited hematocrit range tested in these capillaries and the large scatter of the data points does not allow a thorough evaluation of the observed curvature. For the smallest capillary tested ($D = 3.3 \mu\text{m}$),

the optimized C value falls to <1 , indicating an overproportional increase of viscosity with hematocrit, but there was again no statistically significant difference compared with the C value of a linear fit. We therefore chose to represent the data for all capillaries with diameters from 6 to 3.3 μm with a C value of 1.

The data given in Fig. 4 indicate a sharp transition between single- and multifile flow regimes between tube diameters of 6 and 9 μm . In addition, there is some indication of a minimum of C in the diameter range just above the transition zone.

A hypothetical explanation of these findings can be deduced from the available knowledge of the hematocrit and diameter dependence of the erythrocyte arrangement in tube flow. In tubes of $<6 \mu\text{m}$, erythrocytes will travel in a single-file flow pattern regardless of hematocrit, since only one cell can be accommodated in a given tube cross section. In slightly larger tubes, however, direct observations (20) have shown that single-file flow occurs at low hematocrit, whereas multifile flow conditions prevail at higher hematocrits. In this diameter range, η_{rel} should therefore increase approximately linearly with hematocrit in the low hematocrit range, whereas above a certain threshold viscosity should increase overproportionally. Combining a linear initial with a curved segment would result in a relationship between η_{rel} and Hct_D characterized by lower C values than those determined for larger tubes in which multiflow conditions prevail over most of the hematocrit range. These considerations suggest the use of a two-phase fitting equation to the viscosity-hematocrit relationship that describes the hematocrit threshold at which the transition between the linear and the overproportional domain takes place. However, the available experimental data do not support such a procedure for the investigated diameter range. In most studies, this might be due to the limited hematocrit range covered in the experiments or the low number of data points obtained. But even in the diameter range between 9 and 40 μm , in which the present experimental data provide a large data base (Fig. 3), no sharp transition in the viscosity-hematocrit relationship can be identified and the experimental data are adequately fitted with the continuous Eq. 3.

The present study was aimed at providing an empirical description of experimental data correlating apparent blood viscosity, tube diameter, and hematocrit. This was intended to allow the developments of models simulating blood flow through microvascular networks. Because this compilation demonstrates consistent trends and remarkable agreement, it might also stimulate the development of theoretical concepts for a rheological analysis of apparent blood viscosity in tube flow. A comparison of theoretical predictions with combined experimental results from various studies would provide a better evaluation criterion than those available for theoretical treatments up to date (14, 24, 27, 29, 53, 56).

The authors acknowledge the support by Dr. G. R. Cokelet, Rochester, NY, who provided some earlier unpublished data obtained in cooperation with J. H. Barbee. Helpful discussions with Dr. T. W. Secomb, Tucson, AZ, are gratefully appreciated. We also thank L. Glahé and

M. Ehrlich for technical assistance and A. Scheuermann for help in preparing the manuscript.

This study was in part supported by the Deutsche Forschungsgemeinschaft.

Address for reprint requests: A. R. Pries, Dept. of Physiology, Freie Universität Berlin, Arnimallee 22, D-1000 Berlin 33, FRG.

Received 15 April 1992; accepted in final form 9 July 1992.

REFERENCES

1. Albrecht, K. H., P. Gaehtgens, A. Pries, and M. Heuser. The Fahraeus effect in narrow capillaries (i.d. 3.3 to 11.0 m). *Microvasc. Res.* 18: 33-47, 1979.
2. Azelvandre, F., and C. Oiknine. Effet Fahraeus et effet Fahraeus-Lindqvist: résultats expérimentaux et modèles théoriques. *Biorheology* 13: 325-335, 1976.
3. Barbee, J. H. The effect of temperature on the relative viscosity of human blood. *Biorheology* 10: 1-5, 1973.
4. Barbee, J. H., and G. R. Cokelet. Prediction of blood flow in tubes with diameters as small as 29 μ . *Microvasc. Res.* 3: 17-21, 1971.
5. Barras, J.-P. Relation entre la viscosité sanguine et l'hématocrite. I. *Helv. Physiol. Acta* 23: 16-25, 1965.
6. Barras, J.-P. Relation entre la viscosité sanguine et l'hématocrite. II. *Helv. Physiol. Acta* 23: 97-106, 1965.
7. Barras, J.-P. L'écoulement du sang dans les capillaires. *Helv. Med. Acta* 34: 468-477, 1968.
8. Bayliss, L. E. Rheology of blood and lymph. In: *Deformation and Flow in Biological Systems*, edited by A. Frey-Wissling. Amsterdam: North-Holland, 1952, p. 355-418.
9. Braasch, D. The missing negative effect of red cell aggregation upon blood flow in small capillaries at low shear forces. *Biorheology Suppl.* 1: 227-230, 1984.
10. Braasch, D., and W. Jenett. Erythrozytenflexibilität, Hämkonzentration und Reibungswiderstand in Glaskapillaren mit Durchmessern zwischen 6 bis 50 μ . *Pfluegers Arch.* 302: 245-254, 1968.
11. Brooks, D. E., J. W. Goodwin, and G. V. F. Seaman. Interactions among erythrocytes under shear. *J. Appl. Physiol.* 28: 172-177, 1970.
12. Chien, S., S. Usami, R. J. Dellenback, and C. A. Bryant. Comparative hemorheology—hematological implications of species differences in blood viscosity. *Biorheology* 8: 35-57, 1971.
13. Cokelet, G. R., and H. L. Goldsmith. Decreased hydrodynamic resistance in the two-phase flow of blood through small vertical tubes at low flow rates. *Circ. Res.* 68: 1-17, 1991.
14. Das, R. N., and V. Seshadri. A semi-empirical model for flow of blood and other particulate suspensions through narrow tubes. *Bull. Math. Biol.* 37: 459-470, 1975.
15. Fahraeus, R. Die Strömungsverhältnisse und die Verteilung der Blutzellen im Gefäßsystem. Zur Frage der Bedeutung der intravaskulären Erythrozytenaggregation. *Klin. Wochenschr.* 7: 100-106, 1928.
16. Fahraeus, R., and T. Lindqvist. The viscosity of the blood in narrow capillary tubes. *Am. J. Physiol.* 96: 562-568, 1931.
17. Fenton, B. M., D. W. Wilson, and G. R. Cokelet. Analysis of the effects of measured white blood cell entrance times on hemodynamics in a computer model of a microvascular bed. *Pfluegers Arch.* 403: 396-401, 1985.
18. Furman, M. B., and W. L. Olbricht. Unsteady cell distributions in capillary networks. *Biotechnol. Prog.* 1: 26-32, 1985.
19. Gaehtgens, P. Flow of blood through narrow capillaries: rheological mechanisms determining capillary hematocrit and apparent viscosity. *Biorheology* 17: 183-189, 1980.
20. Gaehtgens, P., C. Duhrssen, and K. H. Albrecht. Motion, deformation, and interaction of blood cells and plasma during flow through narrow capillary tubes. *Blood Cells* 6: 799-812, 1980.
21. Gerstädt, H., C. Vogtmann, P. Rüth, and E. Schöntube. Die Scheinviskosität von Blut in Glaskapillaren kleinsten Durchmessers. *Naturwissenschaften* 53: 526, 1966.
22. Gupta, B. B., and V. Seshadri. Flow of red blood cell suspensions through narrow tubes. *Biorheology* 14: 133-143, 1977.
23. Halikas, G., and C. W. Sheppard. The viscosity of water and of blood in small diameter capillary tubes. Anomalous viscosity of blood. *Biorheology* 6: 137-142, 1969.

24. **Haynes, R. H.** Physical basis of the dependence of blood viscosity on tube radius. *Am. J. Physiol.* 198: 1193–1200, 1960.
25. **Haynes, R. H., and A. C. Burton.** Role of the non-Newtonian behavior of blood in hemodynamics. *Am. J. Physiol.* 197: 943–950, 1959.
26. **Hudetz, A. G., J. G. Spaulding, and M. F. Kiani.** Computer simulation of cerebral microhemodynamics. *Adv. Exp. Med. Biol.* 248: 293–304, 1989.
27. **Isenberg, I.** A note on the flow of blood in capillary tubes. *Bull. Math. Biophys.* 15: 149–152, 1953.
28. **Jay, A. W. L., S. Rowlands, and L. Skibo.** The resistance to blood flow in the capillaries. *Can. J. Physiol. Pharmacol.* 50: 1007–1013, 1972.
29. **Johnson Dix, F., and G. W. Scott Blair.** On the flow of suspensions through narrow tubes. *J. Appl. Phys.* 11: 574–581, 1940.
30. **Kiani, M. F., and A. G. Hudetz.** A semi-empirical model of apparent blood viscosity as a function of vessel diameter and discharge hematocrit. *Biorheology* 28: 65–73, 1991.
31. **Levin, M., B. Dawant, and A. S. Popel.** Effect of dispersion of vessel diameters and lengths in stochastic networks. II. Modeling of microvascular hematocrit distribution. *Microvasc. Res.* 31: 223–234, 1986.
32. **Lipowsky, H. H., S. Kovalcheck, and B. W. Zweifach.** The distribution of blood rheological parameters in the microvasculature of cat mesentery. *Circ. Res.* 43: 738–749, 1978.
33. **Martini, P., A. Pierach, and E. Schreyer.** Die Strömung des Blutes in engen Gefäßen. Eine Abweichung vom Poiseuille'schen Gesetz. *Dtsch. Arch. Klin. Med.* 169: 212–222, 1930.
34. **McKay, C. B., and H. J. Meiselman.** Osmolality mediated Fahraeus and Fahraeus-Lindqvist effects for human erythrocytes suspensions. *Am. J. Physiol.* 254 (Heart Circ. Physiol. 23): H238–H249, 1988.
35. **Neuhaus, D., M. R. Fedde, and P. Gaehtgens.** Changes in haemorheology in the racing greyhound as related to oxygen delivery. *Eur. J. Appl. Physiol.* 65: 278–285, 1992.
36. **Papenfuss, H. D., and J. F. Gross.** Microhemodynamics of capillary networks. *Biorheology* 18: 673–692, 1981.
37. **Papenfuss, H. D., and J. F. Gross.** Mathematical simulation of blood flow in microcirculatory networks. In: *Microvascular Networks: Experimental and Theoretical Studies*, edited by A. S. Popel and P. C. Johnson. Basel: Karger, 1986, p. 168–181.
38. **Pirofsky, B.** The determination of blood viscosity in man by a method based on Poiseuille's law. *J. Clin. Lab. Invest.* 32: 292–298, 1953.
39. **Pries, A. R., K. H. Albrecht, and P. Gaehtgens.** Model studies on phase separation at a capillary orifice. *Biorheology* 18: 355–367, 1981.
40. **Pries, A. R., T. W. Secomb, P. Gaehtgens, and J. F. Gross.** Blood flow in microvascular networks. Experiments and simulation. *Circ. Res.* 67: 826–834, 1990.
41. **Prothero, J. W., and A. C. Burton.** The physics of blood flow in capillaries. II. The capillary resistance to flow. *Biophys. J.* 2: 199–212, 1962.
42. **Reinke, W., P. Gaehtgens, and P. C. Johnson.** Blood viscosity in small tubes: effect of shear rate, aggregation, and sedimentation. *Am. J. Physiol.* 253 (Heart Circ. Physiol. 22): H540–H547, 1987.
43. **Reinke, W., P. C. Johnson, and P. Gaehtgens.** Effect of shear rate variation on apparent viscosity of human blood in tubes of 29 to 94 μm diameter. *Circ. Res.* 59: 124–132, 1986.
44. **Schmid-Schönbein, G. W., R. Skalak, S. Usami, and S. Chien.** Cell distribution in capillary networks. *Microvasc. Res.* 19: 18–44, 1980.
45. **Schofield, R. K., and G. W. Scott Blair.** The influence of the proximity of a solid wall on the consistency of viscous and plastic materials. *J. Phys. Chem.* 34: 248–262, 1930.
46. **Secomb, T. W.** Flow-dependent rheological properties of blood in capillaries. *Microvasc. Res.* 34: 46–58, 1987.
47. **Secomb, T. W., and J. F. Gross.** Flow of red blood cells in narrow capillaries: role of membrane tension. *Int. J. Microcirc. Clin. Exp.* 2: 229–240, 1983.
48. **Secomb, T. W., A. R. Pries, P. Gaehtgens, and J. F. Gross.** Theoretical and experimental analysis of hematocrit distribution in microcirculatory networks. In: *Microvascular Mechanics: Hemodynamics of Systemic and Pulmonary Microcirculation*, edited by J. S. Lee and T. C. Skalak. New York: Springer, 1989, p. 39–49.
49. **Secomb, T. W., R. Skalak, N. Özkaya, and J. F. Gross.** Flow of axisymmetric red blood cells in narrow capillaries. *J. Fluid Mech.* 163: 405–423, 1986.
50. **Skalak, R., P. H. Chen, and S. Chien.** Effect of hematocrit and rouleaux on apparent viscosity in capillaries. *Biorheology* 9: 67–82, 1972.
51. **Stadler, A. A., E. P. Zilow, and O. Linderkamp.** Blood viscosity and optimal hematocrit in narrow tubes. *Biorheology* 27: 779–788, 1990.
52. **Stone, H. O., H. K. Thompson, Jr., and K. Schmidt-Nielsen.** Influence of erythrocytes on blood viscosity. *Am. J. Physiol.* 214: 913–918, 1968.
53. **Thomas, H. W.** The wall effect in capillary instruments: an improved analysis suitable for application to blood and other particulate suspensions. *Biorheology* 1: 41–56, 1962.
54. **Voss, R.** Entwicklung einer kapillarviskosimetrischen Methode zur Untersuchung der Schubspannungsabhängigkeit des Fahraeus-Lindqvist-Effektes (Dissertation). Cologne, FRG: Univ. of Cologne, 1983.
55. **Warnke, K. C., and T. C. Skalak.** The effects of leukocytes on blood flow in a model skeletal muscle capillary network. *Microvasc. Res.* 40: 118–136, 1990.
56. **Whitmore, R. L.** A theory of blood flow in small vessels. *J. Appl. Physiol.* 22: 767–771, 1967.